# 18-Crown-6 and Its Hydrates: Bridging but Versatile Hydrogen Bonding. A Theoretical Study of Static and Dynamic Properties

**R. Schurhammer, P. Vayssière, and G. Wipff***

*UMR 7551 CNRS, Laboratoire MSM, Institut de Chimie, 4 rue Blaise Pascal, 67000 Strasbourg, France*

*Received: July 28, 2003*

Quantum chemical (QM), classical molecular dynamics (MD), and Car−Parrinello (CP-MD) studies are reported for 18-crown-6 (18C6) and its first 18C6$(H_2O)_n$ hydrates, focusing on the $D_{3d}$ and $C_i$ forms of the crown. They reveal the importance of dynamics and the surrounding medium on its conformational and hydrogen-bonding properties. In the gas phase, the two forms of the free crown are found to be quasi-isoenergetic at several computational levels, but during CP-MD simulations, the $D_{3d}$ form is more mobile than $C_i$ and undergoes conformational changes in such a way as "to fill its own cavity". Among several forms of the monohydrate, the one with a $D_{3d}$-type crown and a bridging water molecule is most stable. Along its 10-ps CP-MD trajectory, the $H_2O$ molecule undergoes a "merry-go-round" dynamics, exchanging between the three "top" oxygens of the deformed crown, and is thus more often instantaneously monodentate than bidentate. The static and dynamic results of different forms of the mono- and dihydrates confirm the importance of dynamic bridging coordination to 18C6. These results solve the apparent contradiction between IR spectroscopic results in humid $CCl_4$ or supercritical-$CO_2$ solutions that hint at an equilibrium between monodentate and bidentate hydrogen bonds, whereas in other humid phases (solid-state structures, liquid hydrates, simulated aqueous solutions), the hydrated crown is always $D_{3d}$-like and the first coordinated $H_2O$ molecules are bridging.

## Introduction

Like (poly)cyclic complex-forming molecules,[1,2] 18-crown-6 (18C6) was early recognized to act as a selective host for charged atoms and small molecules and to display fundamental features of molecular recognition: preorganization and macrocyclic effects, flexibility, induced fit upon ligand binding, and a solvent effect on its recognition properties.[3−5] From a basic point of view, it is important to understand the structure of 18C6 as a function of its environment. In the solid state, 18C6 alone is of an elongated shape of $C_i$ symmetry (no cavity), and the $D_{3d}$ form (Figure 1) with a cavity is commonly observed with cationic guests (e.g., $K^+$, $R-NH_3^+$, $H_3O^+$, $NH_4^+$) as well as in interaction with dipolar molecules (e.g., acetonitrile, water).[6−8] Other symmetries are observed for 18C6 itself (e.g., $C_1$ within the $Na^+$ complex, another $C_i$ form in the benzene−sulfonamide adduct) or its derivatives (e.g., dicyclohexyl, dibenzo).[6] These data and computer simulations in the gas phase[9−12] and in solution[13−18] show that the structure of 18C6 is highly versatile and depends on its environment.

The present study was motivated by spectroscopic IR results on 18C6 hydrates formed in humid organic phases such as $CCl_4$[19] or supercritical $CO_2$ (SC -$CO_2$),[20] according to which there is an equilibrium between the monodentate and bidentate coordination of water in the 1:1 adduct with 18C6 (Figure 2). The corresponding conformation of 18C6 was not established. However, early theoretical simulations on 18C6 in aqueous solution showed that among the $C_i$, $C_1$, and $D_{3d}$ forms, the $C_i$ one interacts poorly with water and forms one-center hydrogen bonds only, $C_1$ forms three strong bridging interactions with water, and $D_{3d}$ forms cooperative 2 + 2 bridging interactions. It was also predicted that the dissolution of crystals of 18C6 in water would lead to conformational changes from $C_i$ to $D_{3d}$.[21] This hydration scheme was confirmed experimentally by X-ray structures of 18C6 hydrates[22,23] or of adducts with other species[24,25] by Raman or IR spectroscopic studies of 18C6 hydrates[26−29] as well as by molecular dynamics[30−32] or Monte Carlo[33] simulations in aqueous solution. It was found that the $D_{3d}$ structure becomes increasingly preferred over $C_i$ as the solvent polarity increases.[16,34] To our knowledge, no form other than $D_{3d}$ has been found in solid structures of 18C6/$H_2O$ adducts.[25] The relevance of these results to humid organic phases may be questioned because structures with bridging $H_2O$ molecules seem to be inconsistent with the monodentate coordination indicated from IR results. Another puzzling feature appeared from MD simulations when a piece of a crystal of 18C6 was "dissolved" at a SC-$CO_2$/water interface.[35] During the dynamics, 18C6 molecules diffused into the $CO_2$ phase, most of them undergoing conformational changes from $C_i$ to $D_{3d}$. Some formed bridging hydrogen bonds with dragged $H_2O$ molecules, and others were surrounded by $CO_2$ molecules only. Conformational preferences are generally believed to be similar in apolar solvents as in the gas phase[36] but these MD experiments suggested that is not the case, and the observation of extracted 18C6 $D_{3d}$ ($H_2O$) supermolecules with bridging water again seems to conflict with IR spectroscopic observations of monodentate hydrates.

In this paper, we first address the question of the conformation of 18C6 and its mono- and dihydrates in the gas phase, with a particular focus on the $C_i$ versus $D_{3d}$ forms and on their dynamic properties. Before elucidating the water-binding mode to the crown, it is indeed essential first to assess the conformation of the free crown itself. According to force-field calculations,[9,11] these are close in energy, and the energy minimum depends on the choice of atomic charges and dielectric constant $\epsilon$. The $D_{3d}$

* Corresponding author. E-mail: wipff@chimie.u-strasbg.fr.

10.1021/jp036196h CCC: $25.00 
Published on Web 11/13/2003

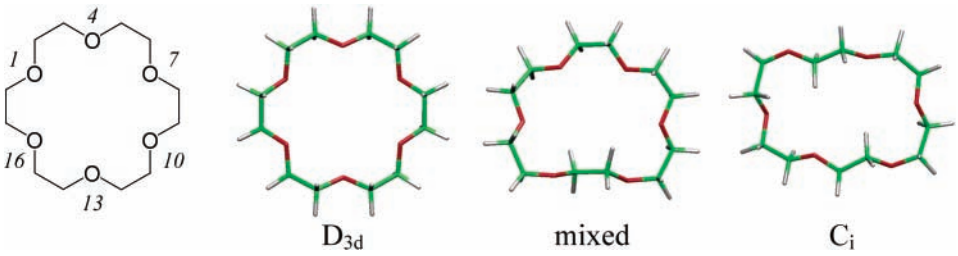


**Figure 1.** Typical forms of 18C6.

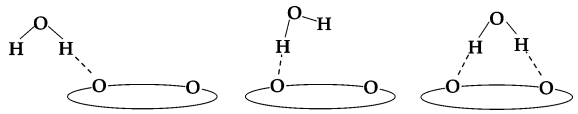

**Figure 2.** Schematic representation of single-*out*, single-*in* (monodendate), and bridging (bidendate) coordination of water to 18C6.

form is stabilized by the internal-energy components (bond + angle + dihedral deformations) but is destabilized by internal electrostatic strain and 1,4 nonbonded interactions between oxygens in the gauche OC−CO arrangements. These empirical results conflict with those of an ab initio QM study at the correlated MP2/6-31G level, according to which $D_{3d}$ is less stable than $C_i$ by 17 kcal/mol, which according to the authors "exclude its existence in the gas phase at room temperature".[37] We notice that this study used force-field instead of quantum mechanical optimized structures. We thus first revisit the energy difference $\Delta E$ between these forms at different computational levels based on QM geometry optimizations. The results are compared with those of AMBER classical molecular mechanics calculations. The second issue concerns the mono- and dihydrates formed by the $C_i$ and $D_{3d}$ forms of the crown, with a particular focus on bridging (bidentate) versus single (monodentate) water coordination. The dynamics features of 18C6 $C_i$ and $D_{3d}$ and their hydrates are studied in the gas phase by Car−Parrinello CP-MD calculations. To investigate the influence of apolar solvents on conformational properties of 18C6 and its hydrates, we performed classical MD simulations in an explicitly represented $CO_2$ solution. These studies provide new insights into the static and dynamic features of 18C6 and its hydrates and allow us to understand how a water molecule bridging over a $D_{3d}$-like crown may appear to form a single hydrogen bond.

## Computational Details

All geometries have been fully optimized at the density-functional theory (DFT) level without symmetry constraints using the 6-31G* basis[38] and the gradient-corrected exchange and correlation functionals according to Becke[39] and Lee, Yang, and Parr[40] (denoted BLYP). This combination of functionals has been shown to perform well for hydrogen-bonded systems.[41] The nature of the stationary points was verified by the computation of the harmonic vibrational frequencies at the BLYP/6-31G* level, which were also used unscaled to obtain thermodynamic corrections to estimate entropies and free energies. Optimization tests with the 6-31G* basis set at the HF, B3LYP, and MP2 levels were also performed. Single-point energy evaluations were performed for the BLYP/6-31G* geometries using the 6-31G* basis set at the HF, B3LYP, or MP2 level as well as with the large 6-311G$^{++}$(3df,3dp) basis set at the HF, B3LYP, and BLYP levels. These computations were carried out with the Gaussian 98 program package.[42] Unless otherwise noted, energies are reported at the BLYP/6-311G$^{++}$(3df,3dp) level employing the BLYP/6-31G* geometries. The calculated interaction energies between $H_2O$ and 18C6 have been systematically corrected for basis-set superposition error (BSSE) by means of the counterpoise method[43] when the 6-31G* basis set was used. Tests on the $D_{3d}$ and $C_i$ forms with the large 6-311G$^{++}$(3df,3dp) basis set showed that this correction is small (<0.5 kcal/mol), thus it has not been reported.

Additional optimizations were performed using the density functional-based Car−Parrinello scheme[44] as implemented in the CPMD program.[45] The BLYP functional combination was employed, together with norm-conserving pseudopotentials generated according to the Martins and Troullier procedure[46] and transformed into the Kleinman−Bylander form (BLYP MT).[47] We also tested the BP86 functional using the same procedure (BP86 MT) as well as the BLYP functional with a dual-space Goedecker pseudopotential (BLYP SG).[48] Periodic boundary conditions were imposed using cubic supercells with a box length of 15 Å. Kohn−Sham orbitals were expanded in plane waves up to a kinetic energy cutoff of 80 Ry. The BLYP/6-31G* geometries were taken as starting points and were reoptimized without symmetry restraints until the maximum gradient was less than $5 \times 10^{-4}$ au (denoted CP-opt).

Car−Parrinello molecular dynamics (CP-MD) simulations were performed starting from the lowest-energy structure using a fictitious electronic mass of 600 au and a time step of 0.121 fs. Unconstrained simulations (NVE ensemble) were performed over 2−10 ps at ca. 300(±30) K.

The classical MD simulations were performed with the AMBER5.0 software,[49] in which internal-energy deformations consist of bond and angle harmonic deformations and dihedral energies. Nonbonded interactions are represented by a sum of pairwise Coulombic and van der Waals interactions (1−6−12 potentiel). The parameters for 18C6 and its hydrates are the same parameters as in ref 35, and unless otherwise indicated, we used ESP-derived atomic charges of Kollman et al.[50] on the crown ($q_O = -0.404$, $q_C = 0.244$, and $q_H = -0.021$e). These were compared with a more polar handmade set ($q_O = -0.50$, $q_C = 0.292$, and $q_H = -0.021$e). The 1···4 electrostatic and van der Waals interactions were scaled down by 2.0. The nonbonded interactions were calculated with a 15-Å cutoff and a reaction field correction for long-range electrostatics. The $H_2O$ and $CO_2$ molecules were represented with the TIP3P[51] and Murthy et al.[52] three-point models, respectively. After energy minimization, MD was run in the gas phase or in $CO_2$ solution in the (NVT) ensemble. The temperature was controlled using the Berendsen weak-coupling method.[53] The $CO_2$ box was the same as the one used in ref 35 to study 18C6 at the SC-$CO_2$/water interface.

## Results

**1. Structure and Dynamics of the $C_i$ and $D_{3d}$ Forms of 18C6.** The $C_i$ and $D_{3d}$ forms of 18C6 were compared with different methodologies, and the main results are summarized in Tables 1 and S1 (Supporting Information). The two forms are found to be very close in energy, and depending on the

**TABLE 1: 18C6 Molecule Relative Energies $\Delta E$ (kcal mol$^{-1}$) of the $C_i$, $D_{3d}$, and Mixed Forms Obtained by Different Methods[a]**

| | method | geometry optimization | energy calculation | ΔE |
|---|---|---|---|---|
| $D_{3d}$ | QM | BLYP/6-31G* | BLYP/6-311G$^{++}$(3df,3pd) | −0.1 |
| | CP | CP-opt | BLYP MT | −0.4 |
| | MM | AMBER | $q_O = -0.4$ | −0.3 |
| $C_i$ | QM | BLYP/6-31G* | BLYP/6-311G$^{++}$(3df,3pd) | (0.0) |
| | CP | CP-opt | BLYP MT | (0.0) |
| | MM | AMBER | $q_O = -0.4$ | (0.0) |
| mixed | QM | BLYP/6-31G* | BLYP/6-311G$^{++}$(3df,3pd) | 0.7 |

[a] A full version of the Table is given as Supporting Information (Table S1).

**TABLE 2: QM Calculations on Dimethyl Ether[a]**

| | $E$ | $\mu$ | $d$(O−C) | $q$(O) | $q$(C) |
|---|---|---|---|---|---|
| BLYP/6-31G*//BLYP/6-31G* | −154.9525 | 1.20 | 1.43 | −0.404 | −0.172 |
| B3LYP/6-31G*//B3LYP/6-31G* | −155.0250 | 1.27 | 1.41 | −0.443 | −0.191 |
| MP2/6-31G*//MP2/6-31G* | −154.5034 | 1.60 | 1.41 | −0.598 | −0.163 |
| HF/6-31G*//HF/6-31G* | −154.0647 | 1.48 | 1.39 | −0.590 | −0.160 |
| MP2/6-31G*//BLYP/6-31G* | −154.5026 | 1.61 | 1.43 | −0.602 | −0.160 |
| MP2/6-31G*//B3LYP/6-31G* | −154.5033 | 1.55 | 1.41 | −0.595 | −0.161 |
| BLYP/6-311G$^{++}$(3df,3pd)//BLYP/6-31G* | −155.0211 | 1.23 | 1.43 | −0.551 | 0.204 |
| B3LYP/6-311G$^{++}$(3df,3pd)//B3LYP/6-31G* | −155.0885 | 1.40 | 1.41 | −0.608 | 0.270 |
| MP2/6-311G$^{++}$(3df,3pd)//MP2/6-31G* | −154.7280 | 1.50 | 1.41 | −0.754 | 0.490 |

[a] Energies ($E$ in hartree), dipole moment ($\mu$ in Debye), optimized O−C distance (Å), and Mulliken charges (e) obtained by different methods.

computational level, their relative energy $\Delta E_{C_i-D_{3d}}$ ranges from +7.2 (MP2/6-31G*//MP2/6-31G* calculation) to −0.1 kcal/mol (BLYP/6-311G$^{++}$(3df,3pd)//BLYP/6-31G* calculation). For BLYP/6-31G*-optimized structures, the calculated $\Delta E_{C_i-D_{3d}}$ energy is somewhat larger with the B3LYP than with the BLYP functional (by 0.7 kcal/mol with the 6-31G* basis set and by 1.1 kcal/mol with the large 6-311G$^{++}$(3df,3pd) basis set), and the choice of the B3LYP versus BLYP functional for the optimization has little influence (0.1 kcal/mol with the 6-31G* basis set). In principle, different thermally populated vibrational modes contribute to relative stabilities, but this correction is also weak ($\Delta G_{vib} = 0.7$ kcal/mol at 300 K) compared to the calculated range of relative stabilities.

Given the importance of internal electrostatic interactions, we decided to determine how the different methods account for the dipole moment $\mu$ of dimethyl ether $CH_3-O-CH_3$, similar to constitutive fragments of 18C6. The results (Table 2) show that with the small 6-31G* or the large 6-311G$^{++}$-(3df,3pd) basis sets the MP2-calculated dipole is clearly exaggerated ($\mu = 1.5$ to 1.6 D compared to $\mu_{exp} = 1.30$ D), and the DFT-B3LYP method yields a somewhat larger $\mu$ than does the BLYP method (by 0.07 to 0.17 D). Reasonable agreement is obtained with the B3LYP/6-31G* and BLYP/6-311G$^{++}$(3df,3pd) methods (1.27 and 1.23 D, respectively), which also yield less-polar oxygens. It is noteworthy that the 6-311G$^{++}$(3df,3pd) basis set yields the smallest $\Delta E_{C_i-D_{3d}}$ energy difference (−0.1 kcal/mol), indicating that the two forms are quasi-isoenergetic in the gas phase. A similar conclusion is obtained from the CP-opt optimized structures calculated with the BLYP MT and BP86 methodologies ($\Delta E_{C_i-D_{3d}} = -0.4$ and −0.7 kcal/mol, respectively) as well as with the AMBER force-field method ($\Delta E_{C_i-D_{3d}} = -0.3$ kcal/mol) with "standard" charges ($q_O = -0.40$e).

The C−O and C−C bonds of the $C_i$ form optimized by different methods can be compared with those observed by X-ray crystallography in the crystal at 100 K (Table 3).[54] They are 0.01−0.02 Å longer than in the crystal, possibly because of thermal effects (apparent bond shortening) in the experimental structure.[54]

**TABLE 3: 18C6 $C_i$ Experimental (Crystal)[54] and Optimized (Gas Phase) Distances (Å).**

| geometry | C−C distances | C−O distances |
|---|---|---|
| *X-ray (100 K)* | *1.506−1.512* | *1.418−1.430* |
| BLYP/6−31 G* | 1.528−1.536 | 1.430−1.442 |
| B3LYP/6−31 G* | 1.518−1.524 | 1.413−1.425 |
| MP2/6-31G* | 1.508−1.515 | 1.418−1.430 |
| CP-MD/BLYP MT[a] | 1.525−1.536 | 1.447−1.455 |

[a] Average distances during the last picosecond of simulation.

When simulated for 2.5 ps by CP-MD, both $C_i$ and $D_{3d}$ forms of 18C6 display dynamic properties. It can be seen from the time evolution of the OC−CO dihedrals and cumulated structures (Figure 3) that the $C_i$ crown retains its overall shape while three OC−CO dihedrals of the $D_{3d}$ crown rapidly (in less than 1 ps) undergo conformational changes from gauche to trans to form a "mixed" structure intermediate between $C_i$ and $D_{3d}$. The higher mobility of the $D_{3d}$ compared to the $C_i$ form has been noted earlier on the basis of classical MD simulations, and it was suggested that this can be a general feature of macro(poly)-cyclic hosts, which tend to deform in such a way as to fill their own cavity.[55] According to BLYP/6-311G$^{++}$(3df, 3pd)//BLYP/6-31G* calculations, this mixed form is only 0.7 kcal/mol higher in energy than the $C_i$ form.

The hydrates (vide infra) have thus been studied with the same methodology (i.e., DFT BLYP/6-311G$^{++}$(3df, 3pd)//BLYP/6-31G* and CP-opt calculations for the static properties and CP-MD BLYP MT calculations for the dynamic properties).

**2. Structure and Dynamics of Monohydrates of the $C_i$ and $D_{3d}$ Forms of 18C6.** The 18C6($H_2O$) monohydrate was studied with the $C_i$ and $D_{3d}$ forms of the crown for which bridging bidentate versus single monodentate types of hydrogen-bonding interactions were considered (Figures 2 and 4). The bridging hydrates were built with "linear" bonds between $H_{wat}$ and the $O_1$ and $O_7$ oxygens of 18C6, but other forms have "bifurcated" bonds (i.e., with one of the water protons equidistant from two OC−CO oxygens). For the monodentate single hydrates, two positions of water were considered, with the "free" proton turned inside (*in*) or outside (*out*) the ring. Upon energy minimization,

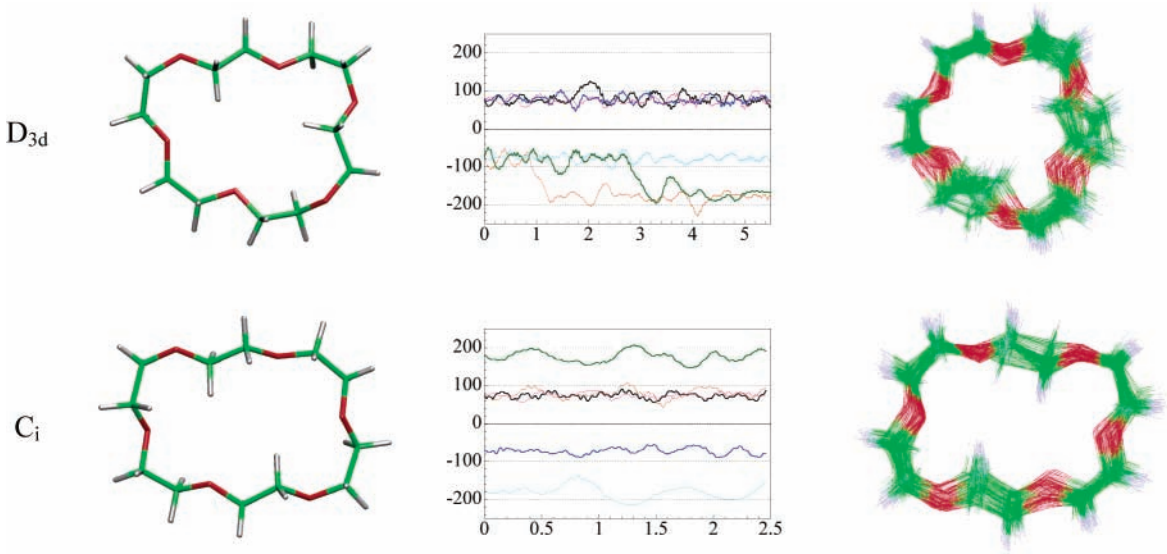


**Figure 3.** Free CP-MD dynamics starting from the $D_{3d}$ vs $C_i$ geometry. From left to right: Final structures, O−C−C−O dihedrals (deg) as a function of time (ps), and cumulated structures.

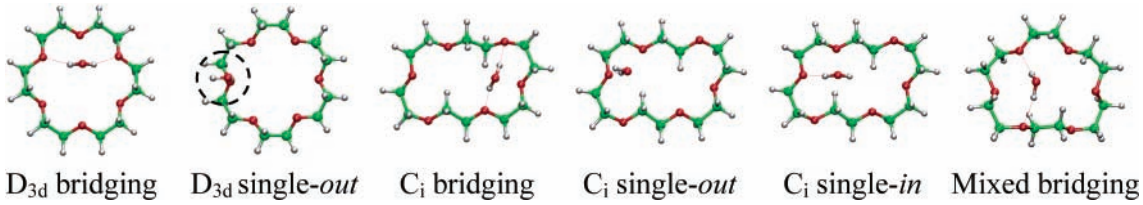


**Figure 4.** 18C6 monohydrate. QM-optimized structures.

**TABLE 4: 18C6 Monohydrate Relative Energies $\Delta E$ (kcal mol$^{-1}$) Obtained with Different Methods**[a]

| | method | geometry optimization | energy calculation | ΔE |
|---|---|---|---|---|
| $D_{3d}$-bridging | QM | BLYP/6-31G* | BLYP/6-311G$^{++}$(3df,3pd) | −2.3 |
| | CP | CP-opt | BLYP MT | −2.2 |
| | MM | AMBER | $q_O = -0.4$ | −1.8 |
| $D_{3d}$-single-*out* | QM | BLYP/6-31G* | BLYP/6-311G$^{++}$(3df,3pd) | 0.6 |
| $C_i$-bridging | QM | BLYP/6-31G* | BLYP/6-311G$^{++}$(3df,3pd) | (0.0) |
| | CP | CP-opt | BLYP MT | (0.0) |
| | MM | AMBER | $q_O = -0.4$ | (0.0) |
| $C_i$-single-*out* | QM | BLYP/6-31G* | BLYP/6-311G$^{++}$(3df,3pd) | 0.7 |
| $C_i$-single-*in* | QM | BLYP/6-31G* | BLYP/6-311G$^{++}$(3df,3pd) | 1.5 |
| mixed bridging | QM | BLYP/6-31G* | BLYP/6-311G$^{++}$(3df,3pd) | 0.3 |

[a] A full version of the Table is given as Supporting Information (Table S2).

the $D_{3d}$-single-*in* form and the $D_{3d}$-bridging bifurcated structures became bridging with linear bonds, and five forms of the monohydrate were finally identified as energy minima: $D_{3d}$-bridging, $D_{3d}$-single-*out*, $C_i$-bridging, $C_i$-single-*out*, and $C_i$-single-*in*. A bridging hydrate of the mixed conformer (mixed bridging) was also optimized (Figure 4). Energies obtained at different computational levels are given in Table S2, and selected results are summarized in Table 4.

*Energy Comparison of the Bridging versus Monodentate Hydrates.* As for 18C6 alone, no unique conclusion is possible concerning the relative stabilities of these hydrates that are close in energy. Taking the $C_i$-bridging structure as a reference, one sees that the $D_{3d}$-bridging structure may be either more stable by <2.6 kcal/mol (HF/6-311G$^{++}$(3df,3pd) calculations) or less stable by up to 3.7 kcal/mol (MP2/6-31G* calculations). However, excluding as above the MP2 results that exaggerate the polarity of the crown and hydrogen bond interactions, and keeping the DFT results with the largest 6-311G$^{++}$(3df,3pd) basis set, yields a preference for the $D_{3d}$-bridging hydrate (by 2.3 kcal/mol). A similar conclusion is obtained from independent CP-opt (BLYP MT) calculations ($\Delta$ = 2.2 kcal/mol) and by AMBER optimizations with standard oxygen charges of −0.40e ($\Delta$ = 1.8 kcal/mol). Increasing these charges to −0.5e favors the $C_i$-bridging form, thus following the same trend in AMBER as in MP2 calculations.

The other structures of the 18C6 monohydrate are slightly less stable than the $C_i$-bridging one ($\Delta$ = 0.6 kcal/mol for $D_{3d}$-single-*out*, 0.7 kcal/mol for $C_i$-single-*out*, 1.5 kcal/mol for $C_i$-single-*in*, 0.6 kcal/mol for $D_{3d}$-single-*out*, and 0.3 kcal/mol for mixed-bridging hydrates (DFT BLYP/6-311G$^{++}$(3df,3pd) energies). In the gas phase, the $D_{3d}$-bridging form is thus more stable than other single and bridging hydrated forms.

Thermal effects on relative stabilities were investigated for the $D_{3d}$- and $C_i$-bridging hydrates, which are the most stable. The former hydrate is more flexible and richer in low vibrational motions than the $C_i$ hydrate and is further stabilized by entropy.

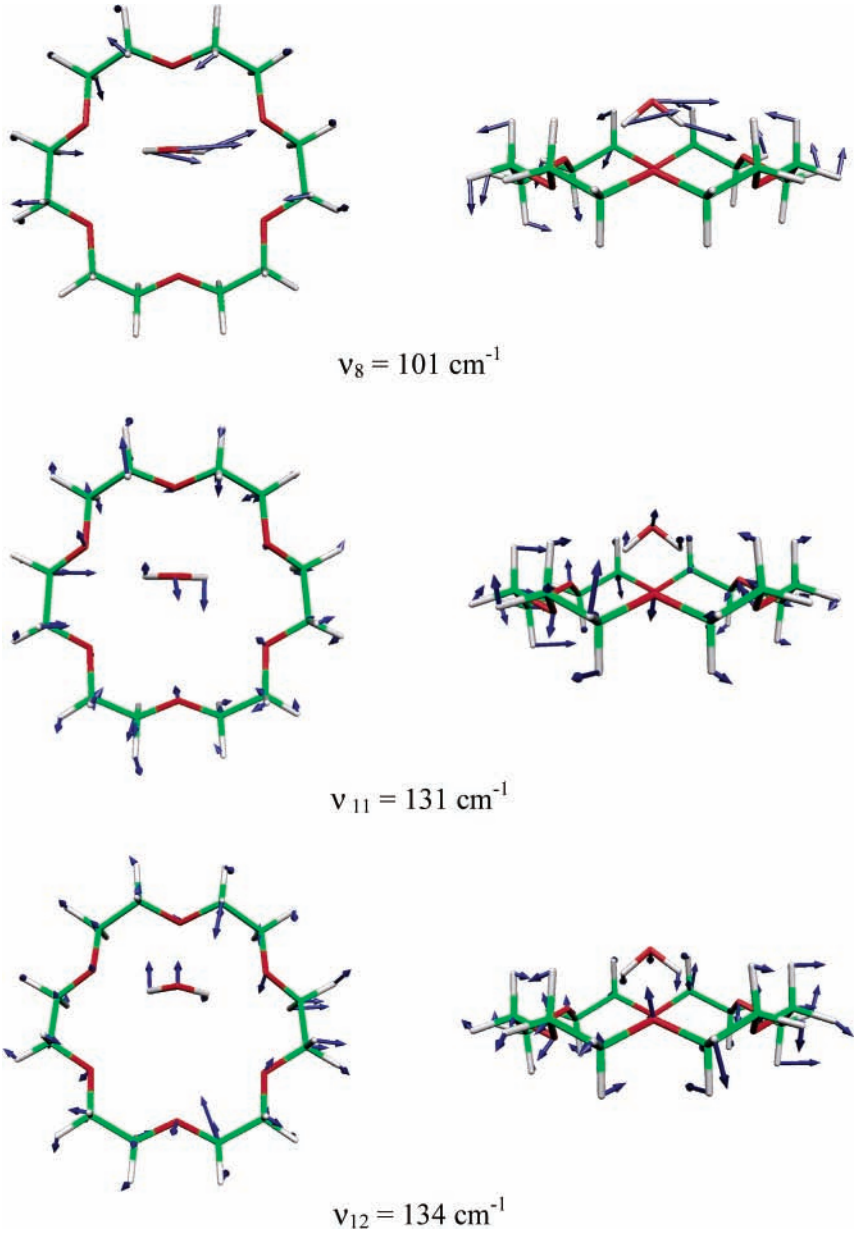


**Figure 5.** Harmonic vibrations of the 18C6 $D_{3d}$ monohydrate. Water motion in the $\nu_8$, $\nu_{11}$, and $\nu_{12}$ low-frequency modes.

The corresponding vibrational entropies are 163 and 159 cal $mol^{-1}$ $K^{-1}$, leading to a further free-energy stabilization of 2.3 kcal/mol at 300 K. Adding this thermodynamic correction to the static energy difference of 2.3 kcal/mol yields a free-energy preference of 4.6 kcal/mol for the $D_{3d}$- over the $C_i$-bridging hydrate.

*Optimized $D_{3d}$-Bridging Hydrate.* Given the large occurrence of bridging hydration in solid-state structures of 18C6,[25] it is interesting to describe the BLYP/6-31G*-optimized $D_{3d}$ hydrate, which interestingly has approximate (pseudo-$C_s$), but not exact $C_s$ symmetry. The $O_{water}$ oxygen is indeed not exactly equidistant from the $O_1$ and $O_7$ oxygens of 18C6 (at 3.063 and 3.039 Å, respectively), leading to $OH\cdots O_{18C6}$ hydrogen bonds of 2.161 and 2.116 Å, which are somewhat longer than usual hydrogen bonds.[56] Optimizations of a $C_s$-symmetrical structure and of other somewhat asymmetrical ones converged to this pseudo-$C_s$ form, which was verified to be a true energy minimum. Depending on whether the $H_2O$ molecule is "anchored" to the $O_1$ or $O_7$ oxygen, there are thus two energy minima separated by a very low symmetrical barrier. The $O_1\cdots O_7$ distance (4.89 Å) is 0.06 Å shorter than in 18C6 $D_{3d}$ itself because of the attractions with water, but 18C6 may not be flexible enough to provide optimal interactions with bridging water.[57]

The representation of the low-frequency vibrational modes of the $D_{3d}$-bridging hydrate (Figure 5) reveals an interesting librational motion ($\nu_8$ at 101 $cm^{-1}$) of the $H_2O$ molecule that oscillates between the $O_1$ and $O_7$ anchoring sites of 18C6. The $\nu_{11}$ and $\nu_{12}$ modes (131 and 134 $cm^{-1}$, respectively) correspond to a rotational motion of $H_2O$ onto the top of the crown. These are precursors of the water dynamics observed in the CP-MD simulations (vide infra).

With regard to hydrogen bonding in the $D_{3d}$- versus $C_i$-bridging hydrates, one sees that the latter is more asymmetrical: one $OH\cdots O_{18C6}$ hydrogen bond is 0.07 Å shorter than in the $D_{3d}$ hydrate, but the other one is similar (2.12 Å). The higher stability of the $D_{3d}$ hydrate relative to the $C_i$ hydrate does not stem from differences in strain energies upon water coordination, however,[58] but mainly from the stronger $H_2O$/18C6 interaction energies (6.1 vs 3.8 kcal/mol, respectively; Table 5).

*On the Strength of Bridging versus Monodentate Hydrogen Bonds.* As expected, monodentate hydrates make shorter O−H·

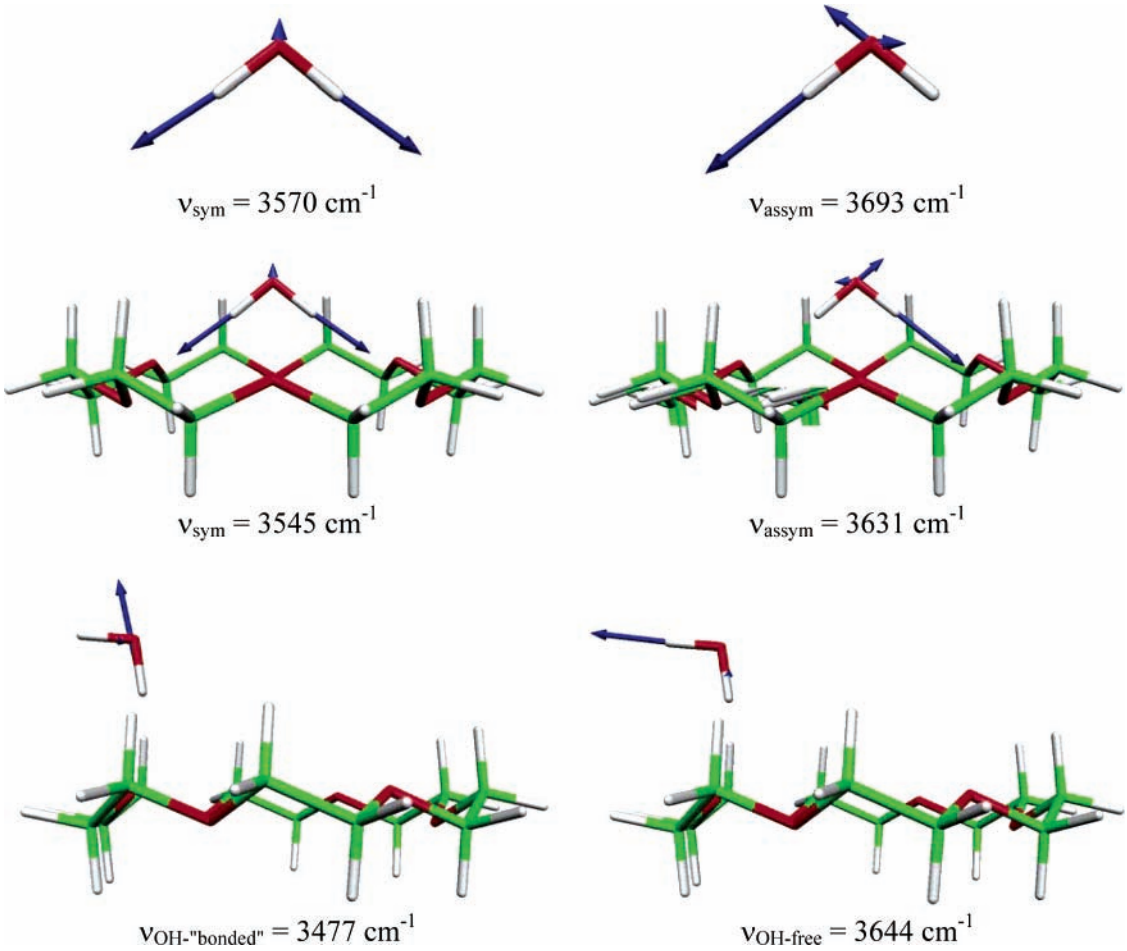


**Figure 6.** Harmonic $\nu_{OH}$ vibrations for $H_2O$ and for the bridging and single-*out* monohydrates of 18C6 $D_{3d}$.

**TABLE 5: 18C6 Monohydrate Interaction Energy (kcal mol$^{-1}$) between 18C6 and $H_2O$ and Characteristic Distances (Å) and Angles (deg)[a]**

| | $D_{3d}$-bridging | $D_{3d}$-single-*out* | $C_{i-}$bridging | $C_{i-}$single-*out* | $C_{i-}$single-*in* | mixed bridging |
|---|---|---|---|---|---|---|
| E(QM)[b] | −6.1 | −3.1 | −3.8 | −2.3 | −3.1 | −4.9 |
| E(CP-opt) | −6.0 | | −4.2 | | | |
| E(AMBER) (300 K) | −5.3 | | | | | |
| E(AMBER) (200 K) | −10.2 | | −5.2 | | | |
| $O_{wat}-H_{wat}$ | 0.983 | 0.988 | 0.985 | 0.986 | 0.986 | 0.984 |
| | 0.983 | 0.980 | 0.984 | 0.979 | 0.979 | 0.984 |
| $O_{wat}\cdots O_{18C6}$ | 3.063 | 2.900 | 3.037 | 2.896 | 2.956 | 2.993 |
| | 3.039 | | 3.090 | | | 3.033 |
| $H_{wat}\cdots O_{18C6}$ | 2.161 | 1.933 | 2.069 | 1.909 | 1.988 | 2.044 |
| | 2.116 | | 2.124 | | | 2.070 |
| $O_{wat}-H_{wat}\cdots O_{18C6}$ | 152 | 165 | 167 | 180 | 167 | 161 |
| | 156 | | 166 | | | 165 |

[a] See structures in Figure 4. [b] BLYP/6-311G$^{++}$(3df,3pd)//BLYP/6-31G* calcualtions.

··O hydrogen bonds than bridging hydrates ($\Delta \approx 0.07-0.13$ Å; Table 5). Following known trends,[59] hydrogen bond weakening corresponds to O−H bond strengthening, and one observes the order of O−H distances: single monodentate hydrogen bond (0.986 to 0.988 Å for the $D_{3d}$-single-*out*, $C_i$-single-*out*, and $C_i$-single-*in* forms) > bridging hydrates (0.983 to 0.985 Å for $D_{3d}$, $C_i$, or mixed crown) > free-OH bond (0.979 Å in the monodentate hydrates and in the isolated $H_2O$ molecule). The O−H vibrational frequencies (cm$^{-1}$) calculated for the bridging- and single-$D_{3d}$ hydrates mirror the evolution from hydrogen-bonded to free-O−H distances: $\nu_{H-bonded}$ (3477 in $D_{3d}$-single-*out*) < $\nu_{sym}$ (3545 in $D_{3d}$-bridging) < $\nu_{asym}$ (3631 in $D_{3d}$-bridging) < $\nu_H$-free (3644 in $D_{3d}$-single-*out*) < $\nu_{asym}$ (3693 in $H_2O$ free). See Figure 6. Clearly, the binding energy of water does not follow the order of hydrogen-bonding distances or O−H vibrational frequencies: it is largest for the $D_{3d}$-bridging hydrate (6.1 kcal/mol) because of cooperative interactions with the crown, and smallest for monocoordinated hydrates (2−3 kcal/mol).

*Dynamic Views of the Bridging Monohydrates in Vacuo.* For the CP-MD simulations, we considered the $C_i$- and $D_{3d}$-bridging forms starting from the energy-minimized structures. Despite their similar energies, these hydrates behave differently; for example, the $C_i$ hydrate was found to dissociate in less than 1 ps at 300 K, but the $D_{3d}$ hydrate remained bound (Figure 7). Its dynamics was pushed up to 10 ps, during which interesting motions were observed. They are pictured by the time evolution of all $H_{wat}\cdots O_{18C6}$ distances and by typical snapshots (Figure

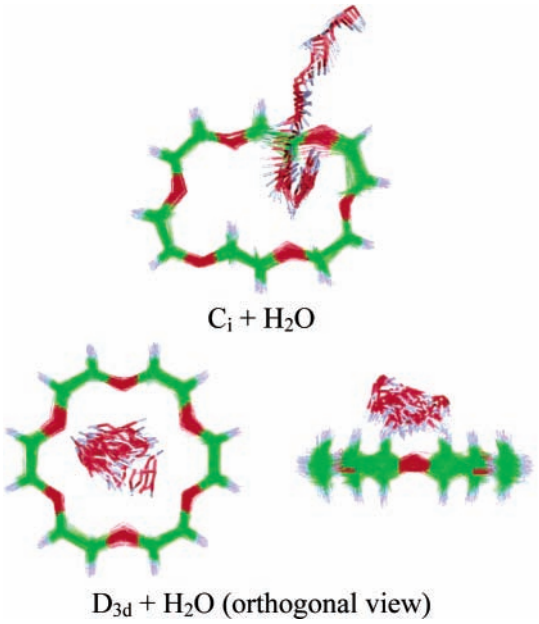


**Figure 7.** CP-MD dynamics of the 18C6 monohydrate: cumulated views of the $C_i$ form (2.5 ps) and $D_{3d}$ form (10 ps).

8). First, one notes that 18C6 $D_{3d}$ is rigidified by water. For 10 ps, it retained its conformation with six gauche OC−CO dihedrals on average and with two distinct triplets of oxygens: $O_1$, $O_7$, and $O_{13}$ point "on top" (i.e., on the water side), and the $O_4$, $O_{10}$, and $O_{16}$ oxygens point to the opposite side (bottom).

The binding mode of the $H_2O$ molecule is highly versatile and dynamic. Schematically, during the first 0.7 ps, $H_2O$ oscillates between $O_1$ and $O_7$, making short contacts of up to 1.65 Å with one oxygen and longer contacts (∼3 Å) with the other one. Between 2.3 and 3.6 ps, it rotates onto the $O_7$ anchor and then onto $O_{13}$ to which it becomes singly hydrogen bonded (1.89 Å at 3.6 ps). A further flip at 5.2 ps leads to transient bridging coordination over $O_1\cdots O_{13}$, followed by a single anchoring to $O_1$ (1.77 Å) at ∼6 ps. The $H_2O$ molecule then anchors to $O_7$ (1.89 Å at ∼6.5 ps), bridges over $O_7\cdots O_{13}$ (2.2 and 2.6 Å) and over $O_{13}\cdots O_1$ (2.6 and 2.0 Å at 8 ps), and finally (at 10 ps) anchors monodentately to $O_1$ (1.87 Å). Thus, the $H_2O$ molecule generally forms one loose monodentate hydrogen bond to one oxygen of the crown (at ∼2.3 ± 0.5 Å), and its other proton oscillates toward the two other top oxygens that are often too remote (>3 Å) to form hydrogen bonds with orbital overlap interactions. The distribution of $O_{18C6}\cdots$HOH distances (Figure 9) peaks at ∼2.2 Å, which corresponds to rather weak hydrogen bonds. In 10 ps, one thus observes the initiation of a "randomized" bridging process over the three pairs of top oxygens of 18C6 $D_{3d}$, reminiscent of the dynamics of $H_3O^+$ with the crown.[60] Dynamic exchange between the three triplets is coupled, but not strictly correlated, with the deformation of 18C6 itself, as seen from the evolution of intracrown $d_{OO}$ distances (Figure 10). The three top and three bottom distances (∼5.1 Å on average) oscillate between 4.5 and 5.6 Å, and only the shorter top ones allow for bridging hydrogen bonds with $H_2O$. During this simulated period, only ∼10% of the structures have $d_{OO}$ distances shorter than 4.7 Å (i.e., the optimal distance in the $(Me_2O)_2\cdots H_2O$ bridging adduct). Also noteworthy is the much weaker occurrence of structures with bidentate $H_2O$ (among the saved 10 000 structures, 15% have two $H_{wat}\cdots O_{18C6}$ distances simultaneously shorter than 2.5 Å) compared to monodentate (67% have only one distance shorter than 2.5 Å). There are thus several processes leading to the dynamics of the bridging $H_2O$: the weakening and loss of one bridging hydrogen bond upon elongation of the O···O anchor of 18C6, the librational motion of water, and water hopping and reorientation, followed by recapture by 18C6. Clearly, this is specific to the $D_{3d}$ adduct in which attractive interactions between the 18C6 quadrupole[61] and the water dipole are retained during the dynamics. The $C_i$ hydrate cannot provide such interactions or hydrogen bonding relays; it thus dissociates during the dynamics.

The results of classical AMBER MD simulations of 50 ps at 300 K on the $C_i$ and $D_{3d}$ hydrates in $CO_2$ solution are consistent with those obtained by CP-MD (Figure S1). The $C_i$ hydrate dissociates, but the $H_2O$ molecule remains dynamically bound to the $D_{3d}$ crown, undergoing excursions to single-*out* coordination to the three top oxygens. At 200 K, the two types of hydrates are stable, and $H_2O$ exchanges between $O_1\cdots O_7$, $O_7\cdots O_{13}$, and $O_1\cdots O_{13}$ bridging positions. When the temperature

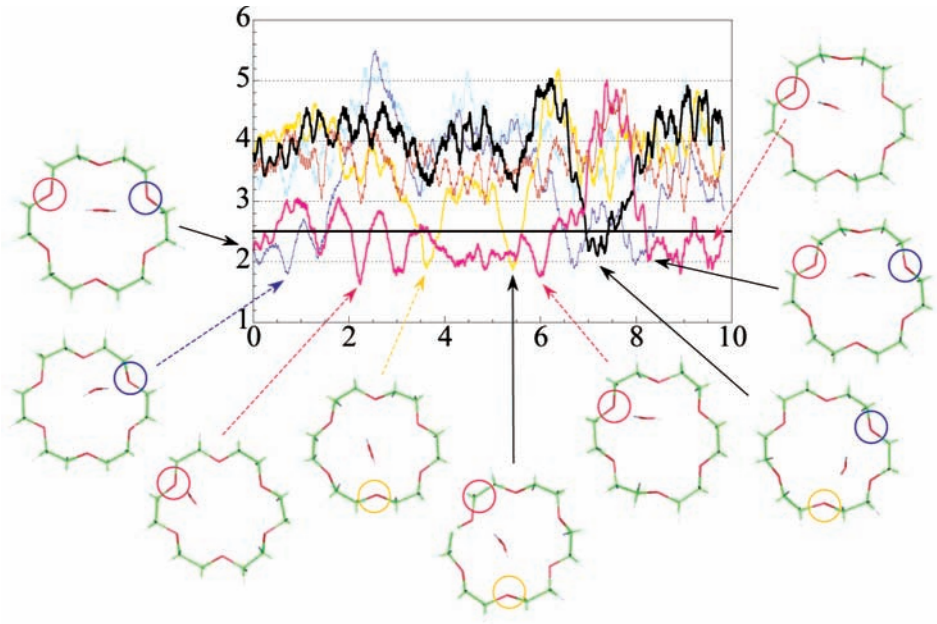


**Figure 8.** CP-MD dynamics of the 18C6 $D_{3d}$ monohydrate. $O_{18C6}\cdots$HOH distances (Å) as a function of time (ps) with selected structures along the trajectory.

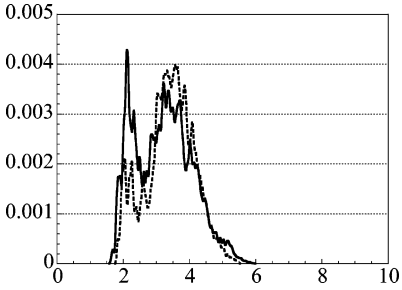


**Figure 9.** CP-MD dynamics of the 18C6 $D_{3d}$ monohydrate. Distribution of $O_{18C6}\cdots HOH$ distances.

is decreased to 100 K, the water molecule sits fixed over $O_1\cdot\cdot\cdot O_7$, without randomizing over the top positions of the crown.

**3. Structure and Dynamics of Dihydrates of 18C6 $D_{3d}$ in Vacuo.** Three forms (I−III) of the 18C6$(H_2O)_2$ dihydrate with a $D_{3d}$-type crown were optimized and simulated for 2.5 ps by CP-MD. They have been built from the monohydrate (with one $H_2O^a$ bridging over the $O_1$ and $O_7$ oxygens of 18C6), to which a second $H_2O^b$ molecule has been added either on the same side (I) or on the opposite side (II and III) of the crown. In dihydrate I, the two $H_2O$ molecules are cooperatively bound, as predicted by theory,[21] and observed in solid-state structures of higher hydrates:[22,23] $H_2O^b$ bridges over the $O_4$ oxygen of 18C6 and the $H_2O^a$ oxygen. In dihydrate II, the $H_2O^b$ molecule has one proton anchored to the $O_4$ oxygen of 18C6, and its other proton bridges over the $O_{10}\cdots O_{16}$ oxygens (Figure 11). In III, $H_2O^b$ relates to $H_2O^a$ via a symmetry-inversion center as in solid-state structures. The optimized structures were similar to the starting ones. Finally, I is found to be more stable than II (by 4.7 kcal/mol) and III (by 2.3 kcal/mol), presumably because the $H_2O^b$ water molecule makes shorter and stronger hydrogen bonds in I (at 1.95 Å with $O_{18C6}$ and 1.87 Å with the

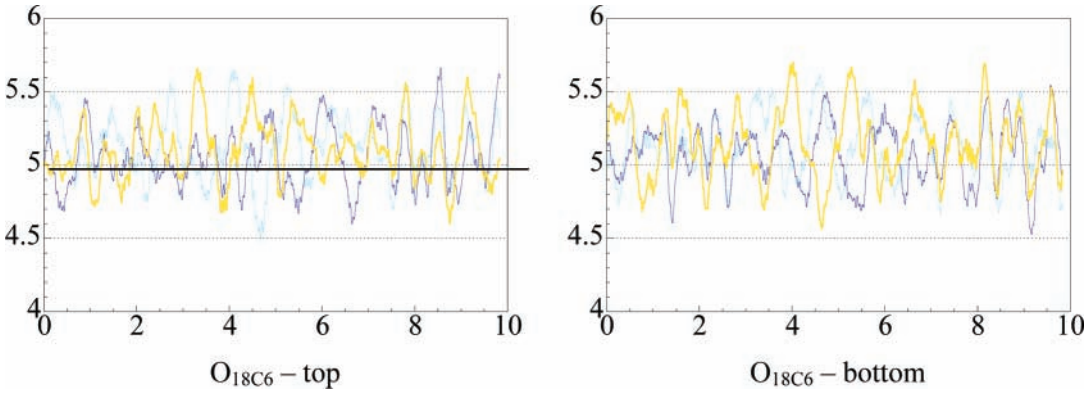


**Figure 10.** CP-MD dynamics of the 18C6 $D_{3d}$ monohydrate. $O_{18C6}\cdots O_{18C6}$ distances (Å) as a function of time (ps).

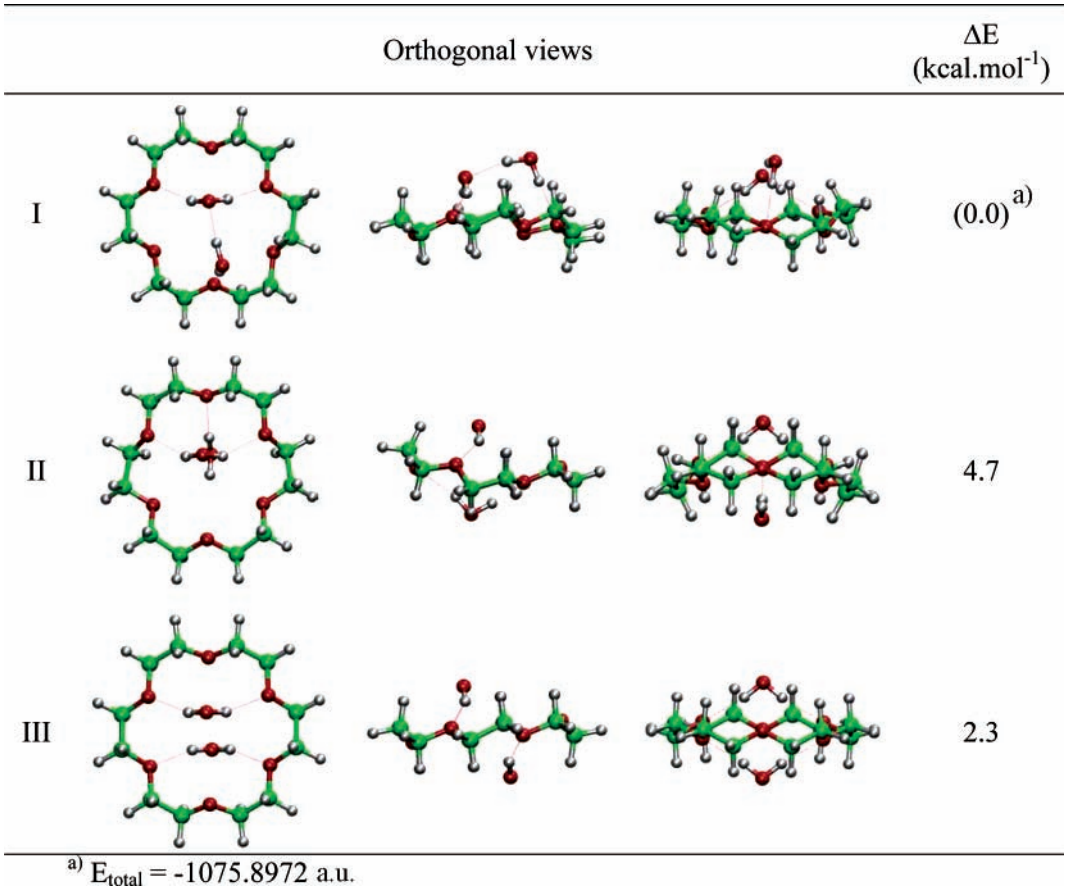


**Figure 11.** QM-optimized 18C6 $D_{3d}$ dihydrate (structures I to III) and relative BLYP/6-311G$^{++}$(3df,pd) energies.

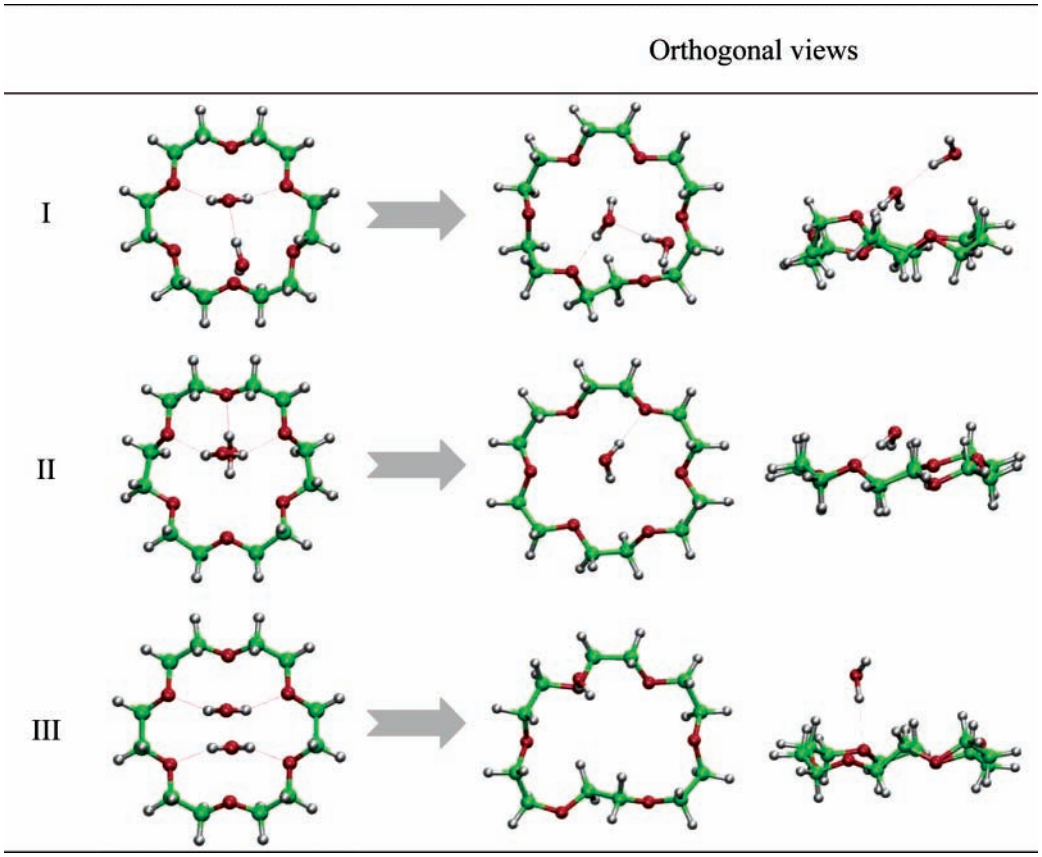


**Figure 12.** CP-MD dynamics of 18C6 $D_{3d}$ dihydrates I to III. Initial and final structures (after 2 ps).

$H_2O^a$ oxygen) than in the other adducts (2.01 Å in I and 2.09 Å in III). Structure II is destabilized by poorer hydrogen-bonding interactions of the bottom $H_2O^b$ molecule that displays long bifurcated ($OH\cdots O_{18C6} = 3.22$ Å) hydrogen bonds with two $O_{18C6}$ oxygens (Figure 11).

None of these structures remained stable during 2 ps of CP-MD simulation (Figure 12). The $H_2O^b$ molecule decomplexed from II and III, and in I it moved from bridging to monocoordination to $H_2O^a$. This is likely due to the deformation of 18C6, which can hardly accommodate two bridging water molecules simultaneously. In III, the remaining $H_2O^a$ molecule is finally monodentate instead of bridging, in relation to the large deviation of the crown from $D_{3d}$ to a mixed shape (Figure 12). The singly hydrogen-bonded water molecules in I are expected to dissociate further from the complex, leaving one bridging monohydrate as described in above. Thus, in the gas phase, dihydrates are unlikely to form with the $D_{3d}$ form of 18C6 and a fortiori with the $C_i$ form.

## Discussion and Conclusions

We have presented a quantum mechanical study of the static and dynamic features of $H_2O$ binding with 18-crown-6. First, according to the QM, CP-opt, and MM results, the $D_{3d}$ form of the free crown is quasi-isoenergetic with the $C_i$ form in the gas phase. These conclusions differ from those of ref 37, where the $D_{3d}$ form was precluded in the gas phase, but agree with those of early force-field calculations.[9,11]

As concerns the hydrates, the results point to the importance of the $D_{3d}$ crown and of bridging water, as observed in solid-state structures and by simulations in water solution. Among the $C_i$ and $D_{3d}$ monohydrates we studied, the $D_{3d}$-bridging monohydrate is energetically preferred mainly because of stronger 18C6/$H_2O$ interactions. The corresponding mimimum-energy structure in which water is bidentate seems to conflict with the spectroscopic observation of an equilibrium between monodentate and bidentate hydrogen bonds,[19] thus raising the question of the nature of the monodentate forms. On the theoretical side, one should in principle sample all possible conformers of the crown interacting with water, which is presently not possible with CP-MD. Kollman et al. showed that long simulations (several nanoseconds) at high temperature were needed to sample the conformational space of 18C6 in the gas phase and that a larger number of conformers were within a few kcal/mol from the absolute minimum.[11] One cannot thus preclude that in the gas phase monodentate hydrates exist in crown conformers other than the $D_{3d}$ and $C_i$ conformers that we considered. (See, for instance, the mixed conformer in Figure 12.) As mentioned in the Introduction, there is, however, good spectroscopic and theoretical evidence for a $D_{3d}$ crown in humid media. It is worth noting that solid-state structures of 18C6 hydrates contain several (4,[23] 6,[22] 8[23]) water molecules and that humid extraction systems (e.g., $CCl_4$ or SC-$CO_2$) contain monohydrates,[19] which hints at the role of second-shell coordination and long-range interactions in the nature of the first hydrates. To our knowledge, in no crystal structure is water coordinated monodentately to the crown.

We believe that our CP-MD and MD results reconcile this apparent paradox. They confirm the stability of the $D_{3d}$-bridging hydrate that remains bound to a $D_{3d}$-like crown. This contrasts with the rapid dissociation of the $C_i$ hydrate in which the water molecule is well bound, and with the conformational instability of the $D_{3d}$ form of free 18C6, thus showing the stabilizing role of the complexed water molecule. According to our CP-MD results, the $D_{3d}$-bridging monohydrate may form upon water dissociation from dihydrates. During the simulated 10-ps period, the water molecules bridging over the $D_{3d}$-like crown are very

dynamic and librate between two top oxygens of the crown in $i\cdots i + 7$ positions, being coordinated most of the time monodentately to only one of them and sometimes "catching" another one via its free OH proton. It is thus essential to consider temperature-dependent nonequilibrium structures in addition to the energy minima only. The $D_{3d}$-bridging hydrate has the lowest energy and should be the most populated at low temperatures. However, its dynamics mainly involves monodentately coordinated water whose proportion should increase with the temperature. This is fully consistent with the IR spectral analysis of Moyer et al.[19] Furthermore, the order of O−H stretching frequencies, calculated on optimized monodentate and bidentate hydrates, is fully consistent with their analysis, according to which $\nu$(OH bridging) > $\nu$(OH monodentate), thus following the order opposite to the total energies and to the water-binding energies.

The agreement between gas-phase calculated and experimental results obtained in apolar media suggests that the solvent has little influence. This is also supported by the comparison of CP-MD results in vacuo and classical MD results in $CO_2$ solution. An apolar solvent may, however, influence conformational trends, as suggested by the calculated average solute/$CO_2$ interactions energies. For instance, the $D_{3d}$ form of the free 18C6 crown displays better interactions with the solvent than the $C_i$ form (−16.9 vs −21.5 kcal/mol, respectively, mostly of van der Waals origin because of differences in solvent accessible surfaces).[62] Comparing the $D_{3d}$ versus $C_i$ bridging monohydrates, they display similar interactions with $CO_2$ (−20.9 vs −21.9 kcal/mol at 250 K and −42.6 vs −43.3 kcal/mol at 100 K).[63] We notice the increased interaction with the solvent when the temperature decreases, which is due to tighter contacts and longer residence times of the solvent, but the solvation preference for the $D_{3d}$ hydrate is small, thus confirming the convergent views on hydrogen bonding to 18C6 in the gas phase versus apolar solution. In aqueous environments, as in solid-state structures of hydrates, the situation differs as the "merry-go-round" dynamics of the bridging water molecule is prevented by its additional coordination to other polar molecules or metals, and water bridges on both sides on the rigid crown.

Finally, on the methodological side, it is worth noting that once the computationally demanding QM and CP-MD calculations have been completed it is quite gratifying to observe that very cheap force-field-based calculations with standard procedures yield similar conclusions, as far as the relative stabilities of the different forms of the crown and of their hydrates are compared.

**Acknowledgment.** We are grateful to IDRIS, CINES, Université Louis Pasteur, and PARIS for computer resources. W.G. thanks Dr. B. Moyer for stimulating discussions.

**Supporting Information Available:** 18C6 $D_{3d}$ and $C_i$ monohydrates simulated by MD with AMBER in $CO_2$ solution with a rigid crown. This material is available free of charge via the Internet at http://pubs.acs.org.

## References and Notes

(1) Lehn, J. M. *Acc. Chem. Res.* **1978**, *11*, 49−57.
(2) Lehn, J. M. *Angew. Chem., Int. Ed. Engl.* **1988**, *27*, 89−112.
(3) Pedersen, C. J. *J. Am. Chem. Soc.* **1967**, *89*, 7017.
(4) de Jong, F.; Reinhoudt, D. N. *Stability and Reactivity of Crown Ether Complexes.*; Academic Press: New York, 1981.
(5) Moyer, B. A. In *Molecular Recognition: Receptors for Cationic Guests*; Atwood, J. L., Davies, J. E. D., McNicol, D. D., Vögtle, F., Lehn, J.-M., Ed.; Pergamon Press: New York, 1996; pp 325−365 and references therein.
(6) Dobler, M. *Ionophores and Their Structures.*; Wiley-Interscience: New York, 1981.
(7) Dale, J. *Isr. J. Chem.* **1980**, *20*, 3−11.
(8) Fyles, T.; Gandour, R. *J. Inclusion Phenom. Mol. Recognit. Chem.* **1992**, *12*, 313−332.
(9) Wipff, G.; Weiner, P.; Kollman, P. A. *J. Am. Chem. Soc.* **1982**, *104*, 3249−3258.
(10) Billeter, M.; Howard, A. E.; Kuntz, I. D.; Kollman, P. A. *J. Am. Chem. Soc.* **1988**, *110*, 8385−8391.
(11) Sun, Y.; Kollman, P. A. *J. Comput. Chem.* **1992**, *12*, 33−40.
(12) Jagannadh, B.; Kunvar, A. C.; Thangavelu, R. P.; Osawa, E. *J. Phys. Chem.* **1996**, *100*, 14339−14342.
(13) Straatsma, T. P.; McCammon, J. A. *J. Chem. Phys.* **1989**, *91*, 3631−3637.
(14) Ha, Y. L.; Chakraborty, A. K. *J. Phys. Chem.* **1991**, *95*, 10781−10787.
(15) Ha, Y. L.; Chakraborty, A. K. *J. Phys. Chem.* **1991**, *95*, 10781−10787.
(16) Troxler, L.; Wipff, G. *J. Am. Chem. Soc.* **1994**, *116*, 1468−1480.
(17) Leuwerink, F. T. H.; Briels, W. J. *J. Phys. Chem. B* **1997**, *101*, 1024−1034.
(18) Leuwerink, F. T. H.; Briels, W. J. *J. Phys. Chem.* **1995**, *99*, 16549−16557.
(19) Bryan, S. A.; Willis, R. R.; Moyer, B. A. *J. Phys. Chem.* **1990**, *94*, 5230−5233.
(20) Wai, C. M.; Rustenholtz, A. Private communication.
(21) Ranghino, G.; Romano, S.; Lehn, J. M.; Wipff, G. *J. Am. Chem. Soc.* **1985**, *107*, 7873−7877.
(22) Mootz, D.; Albert, A.; Schaefgen, S.; Stäben, D. *J. Am. Chem. Soc.* **1994**, *116*, 12045−12046.
(23) Albert, A.; Mootz, D. *Z. Naturforsch., B* **1997**, *52*, 615−619.
(24) Nordlander, E. H.; Burns, J. H. *Inorg. Chim. Acta* **1986**, *115*, 31−36.
(25) In the *Cambridge Crystallographic Database*, 62 structures are found with 18C6 and $H_2O$. In all of them, the water molecule is bridging over a $D_{3d}$ crown.
(26) Matsuura, H.; Fukuhara, K.; Ikeda, K.; Tachikake, M. *J. Chem. Soc., Chem. Commun.* **1989**, 1814−1816.
(27) Fukuhara, K.; Tachikake, M. *J. Phys. Chem.* **1995**, *99*, 8617−8623.
(28) Patil, K. J.; Pawar, R. B. *J. Phys. Chem. B* **1999**, *103*, 2256−2261.
(29) Patil, K. J.; Pawar, R. B. *Spectrochim. Acta* **2003**, *59*, 1289−1297.
(30) Wipff, G.; Troxler, L. In *Computational Approaches in Supramolecular Chemistry*; Wipff, G., Ed.; Kluwer: Dordrecht, The Netherlands, 1994; pp 319−348.
(31) Kowall, T.; Geiger, A. *J. Phys. Chem.* **1994**, *98*, 6216−6224.
(32) Sun, Y.; Kollman, P. A. *J. Chem. Phys.* **1992**, *97*, 5108−5112.
(33) Krongsuk, S.; Kerdcharoen, T.; Hannongbua, S. *J. Phys. Chem. B* **2003**, *107*, 4175−4181.
(34) Ha, Y. L.; Chakraborty, A. K. *J. Phys. Chem.* **1994**, *98*, 11193−11203.
(35) Vayssière, P.; Wipff, G. *Phys. Chem. Chem. Phys.* **2003**, *5*, 127−135.
(36) Leuwerink, F. T. H.; Briels, W. J. *J. Chem. Phys.* **1995**, *103*, 4637−4652.
(37) von Szentpaly, L.; Shamovsky, I. L. *J. Mol. Struct.: THEOCHEM* **1994**, *305*, 249−260.
(38) Hehre, W. J.; Radom, L.; Schleyer, P.; Pople, J. *Ab Initio Molecular Orbital Theory*; Wiley: New York, 1986.
(39) Becke, A. D. *Phys. Rev. A* **1988**, *38*, 3098−3100.
(40) Lee, C.; Yang, W.; Parr, R. G. *Phys. Rev. B* **1988**, *37*, 785−789.
(41) Sprik, M.; Hutter, J.; Parrinello, M. *J. Chem. Phys.* **1996**, *105*, 1142−1152.
(42) Frisch, M. J.; Trucks, G. W.; Schlegel, H. B.; Scuseria, G. E.; Robb, M. A.; Cheeseman, J. R.; Zakrzewski, V. G.; Montgomery, J. A., Jr.; Stratmann, R. E.; Burant, J. C.; Dapprich, S.; Millam, J. M.; Daniels, A. D.; Kudin, K. N.; Strain, M. C.; Farkas, O.; Tomasi, J.; Barone, V.; Cossi, M.; Cammi, R.; Mennucci, B.; Pomelli, C.; Adamo, C.; Clifford, S.; Ochterski, J.; Petersson, G. A.; Ayala, P. Y.; Cui, Q.; Morokuma, K.; Malick, D. K.; Rabuck, A. D.; Raghavachari, K.; Foresman, J. B.; Cioslowski, J.; Ortiz, J. V.; Stefanov, B. B.; Liu, G.; Liashenko, A.; Piskorz, P.; Komaromi, I.; Gomperts, R.; Martin, R. L.; Fox, D. J.; Keith, T.; Al-Laham, M. A.; Peng, C. Y.; Nanayakkara, A.; Gonzalez, C.; Challacombe, M.; Gill, P. M. W.; Johnson, B. G.; Chen, W.; Wong, M. W.; Andres, J. L.; Head-Gordon, M.; Replogle, E. S.; Pople, J. A. *Gaussian 98*, revision A.5; Gaussian, Inc.: Pittsburgh, PA, 1998.
(43) Boys, S. F.; Bernardi, F. *Mol. Phys.* **1970**, *19*, 553−566.
(44) Car, R.; Parrinello, M. *Phys. Rev. Lett.* **1985**, *55*, 2471−2474.
(45) Hutter, J.; Alavi, A.; Deutsch, T.; Bernasconi, M.; Goedecker, S.; Marx, D.; Tuckerman, M.; Parrinello, M. *Max-Planck-Institut für Festkörperforschung and IBM Research Laboratory*, **1995**−**1999**.
(46) Troullier, N.; Martins, J. L. *Phys. Rev. B* **1991**, *43*, 1993−2006.
(47) Kleinman, L.; Bylander, D. M. *Phys. Rev. Lett.* **1982**, *48*, 1425−1428.

(48) Goedecker, S.; Teter, M.; Hutter, J. *Phys. Rev. B* **1996**, *54*, 1703−1710.

(49) Case, D. A.; Pearlman, D. A.; Caldwell, J. C.; Cheatham, T. E., III; Ross, W. S.; Simmerling, C. L.; Darden, T. A.; Merz, K. M.; Stanton, R. V.; Cheng, A. L.; Vincent, J. J.; Crowley, M.; Ferguson, D. M.; Radmer, R. J.; Seibel, G. L.; Singh, U. C.; Weiner, P. K.; Kollman, P. A. *AMBER5*: University of California: San Francisco, CA, 1997.

(50) Singh, U. C.; Kollman, P. A. *J. Comput. Chem.* **1984**, *5*, 129−145.

(51) Jorgensen, W. L.; Chandrasekhar, J.; Madura, J. D.; Impey, R. W.; Klein, M. L. *J. Chem. Phys.* **1983**, *79*, 926−936.

(52) Murthy, C. S.; Singer, K.; McDonald, I. R. *Mol. Phys.* **1981**, *44*, 135−143.

(53) Berendsen, H. J. C.; Postma, J. P. M.; van Gunsteren, W. F.; DiNola, A. *J. Chem. Phys.* **1984**, *81*, 3684−3690.

(54) Maverick, P.; Seiler, P.; Schweitzer, B.; Dunitz, J. D. *Acta Crystallogr., Sect. B* **1980**, *36*, 615.

(55) Wipff, G.; Wurtz, J. M. In *Transport through Membranes, Carriers, Channels and Pumps.*; Pullman, A., Jortner, J., Pullman, B., Ed.; Dordrecht, The Netherlands, 1988; p 1.

(56) Jeffrey, G. A.; Saenger, W. *Hydrogen Bonding in Biological Structures*; Springer-Verlag: Berlin, 1991.

(57) This can be seen from a comparison between 18C6 $D_{3d}$-bridging and $Me_2O\cdots HOH\cdots OMe_2$ optimized systems. In the latter, (i) the $Me_2O\cdots OMe_2$ distance (4.68 Å) and the $HOH\cdots OMe_2$ hydrogen bond distance (1.986 Å) are somewhat shorter than in the 18C6 $D_{3d}$-bridging hydrate (4.89 and 2.12−2.16 Å, respectively). (ii) The $O_{wat}-H\cdots OMe_2$ angle (162°) is more linear than the $O_{wat}-H\cdots O18C6$ angles (152° and 156°). (iii) The $H_2O$ interaction energy with the two ethers is somewhat larger than with 18C6 $D_{3d}$ (6.4 and 6.1 kcal/mol, respectively; BLYP/6-31G* calculations).

(58) The energy difference between 18C6 free and 18C6 hydrated crowns amounts to 0.7 and 0.3 kcal/mol for the $C_i$ and $D_{3d}$ forms, respectively, which indicates that the deformation energies upon water coordination are small.

(59) Jeffrey, G. A. *An Introduction to Hydrogen Bonding*; Oxford University Press: New York, 1997.

(60) Bühl, M.; Wipff, G. *J. Am. Chem. Soc.* **2002**, *124*, 4473−4480.

(61) Pingale, S. S.; Gadre, S. R.; Bartolotti, L. J. *J. Phys. Chem. A* **1998**, *102*, 9987−9992.

(62) These energies were calculated with a frozen solute to avoid conformational changes of the crown at 300 K.

(63) These energies were calculated with a frozen crown and at low temperature to prevent the dissociation of the water molecule.